Pore-Scale Imaging of Tetrahydrofuran-Hydrate Bearing Porous Media

Mandy Schindler*, Michael Batzle[†] and Manika Prasad, Center for Rock Abuse, Colorado School of Mines

SUMMARY

Naturally occurring gas hydrates contain significant amounts of natural gas which might be produced in the foreseeable future. Thus, it is necessary to understand the pore-space characteristics of hydrate reservoirs, especially the pore-scale distribution of hydrates and their interaction with the sediment. The goal of this study is to determine how the hydrates are distributed in the pore space and the implications of this pore-scale distribution for hydrate saturation estimates from seismic and acoustic velocities.

Laboratory measurements were conducted to obtain information about the distribution of hydrates in the pore space of synthetic sediments (glass beads). Tetrahydrofuran (THF) was used as a guest molecule since THF hydrate is a proxy for naturally occuring hydrate. We performed micro X-ray computed tomography (MXCT) on laboratory formed glass-bead samples. MXCT images indicate that THF hydrates form in the pore space with little to no contact to the grain surfaces. We observed salt precipitation at grain contacts and in small pore space. These hydrate-bearing sediments appear to follow a pore-filling model but contained salt cement. Based on this knowledge, it may be possible to calibrate seismic and well logging data to calculate the amount of natural gas stored in a hydrate reservoir. This information will help to make decisions regarding the producibility of methane hydrates and to develop safe production schemes.

INTRODUCTION

Gas hydrates are clathrate structures of natural gases. They require low temperatures and high pressures for stability. These conditions are met in shallow sediments in Arctic permafrost regions and beneath the seafloor along continental slopes. The estimated amount of natural gas, mainly methane, stored in hydrate reservoirs exceeds the amount of natural gas stored in conventional resources by at least one order of magnitude (Meyer, 1981; Dobrynin et al., 1981; Collett et al., 2009). The widespread occurence of gas hydrates in permafrost and shallow marine sediments is well established (Collett et al., 2009). Anderson et al. (2008) and Dallimore et al. (2008) demonstrated that gas-hydrate production can be developed with existing oil and gas production technology. For successful production of methane gas from hydrate reservoirs we need to obtain knowledge about physical properties of gas-hydrate bearing sediments.

The most common geophysical methods used to characterize and quantify gas hydrates in nature are seismic surveying and well logging. In order to calibrate and interpret these field measurements, laboratory studies are necessary to determine the bulk physical properties of hydrate-bearing sediment. Currently, it is possible to predict the existence of gas hydrates from geophysical measurements. However, the techniques used to estimate hydrate saturation based on either seismic data or well logs require further development (Collett and Lee, 2012). Thus, the amount of hydrates stored in a reservoir remains uncertain in some cases. Information about the distribution of gas hydrates in the rock is necessary to determine hydrate saturation.

Gas hydrates occur as massive units and lenses in fractures of fine-grained material (shale) as well as distributed in the pore space of coarse-grained porous media. Different distributions of gas hydrates in the pore space affect the physical properties of the hydrate-bearing sediment. Thus, it is imperative to ascertain hydrate-sediment interactions rather than physical properties of pure hydrates (Yun et al., 2005). Hydrate distribution in the pore space depends mainly on the formation method. In nature, gas hydrates are formed in two ways: (1) from methane dissolved in water or (2) from free methane gas (Collett et al., 2009). Hydrates formed from methane gas tends to form at the grain surface and grain contacts (Waite et al., 2004; Priest et al., 2005) while hydrates formed from methane dissolved in water tends to form in the pore body with little or no contact to the sediment grains (Ecker et al., 1998; Kunerth et al., 2001).

In this study, we focus on the pore-scale distribution of gas hydrates in synthetic coarse-grained porous media. Coarse grained sand reservoirs, as they exist in permafrost regions and marine environments, are relatively easy to access and thus more likely to permit methane production from gas hydrates than hydrate reservoirs in shale (Boswell and Collett, 2006).

Our goal is to determine the pore-scale distribution of hydrates formed from gas dissolved in water. It is often assumed that gas hydrates in coarse grained, marine sediments is more likely to form from methane dissolved in water, whereas gas hydrates in permafrost regions is associated with formation from free methane gas (Collett et al., 2009). Micro X-ray computed tomography (MXCT) images were utilized to image hydrate distribution in the pore space. The relation between pore-scale distribution, hydrate formation method and seismic or sonic velocities is essential to determine the amount of hydrates in a reservoir from seismic data and acoustic logs.

THEORY

Theoretical models infer different pore-scale hydrate distributions and their impact on seismic velocities. One such model is the effective medium theory applied to hydrate-bearing sediments by Ecker et al. (1998) and Helgerud et al. (1999) .

Figure 1 shows four different pore-scale distributions according to this effective medium model for gas hydrates in sediment: contact cementing, envelope cementing, pore filling and
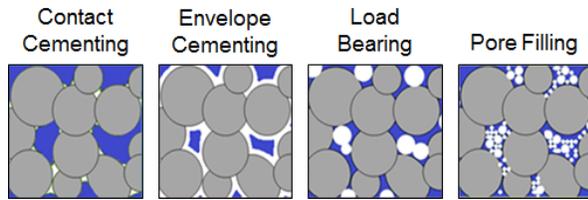
Figure 1: Effective medium theory after Ecker et al. (1998) and Helgerud et al. (1999): different distributions of hydrates in the pore space, conceptual figures from Rydzy and Batzle (2011)

load bearing. The envelope cementing model causes a drastic increase in velocities even for small amounts of hydrates in the pore space whereas hydrates formed according to the pore filling model shows a much smaller influence on velocities. Ultrasonic velocity measurements have been performed in addition to MXCT imaging as discussed in Schindler and Batzle (2014). Hydrate formation from free gas appears to create grain-cementing hydrates, which resembles the contact or envelope-cementing models (Waite et al., 2004; Priest et al., 2005). Hydrates formed from gas dissolved in water seems to have little or no contact with the sediment grains and thus conforms to the load-bearing or pore-filling model (Kerkar et al., 2014). More laboratory measurements are necessary to determine the correlation of hydrate distribution in the pore space with seismic velocities and to corroborate previous results.

The most common hydrates in nature are methane hydrates. Methane hydrates either need to be cooled to -78.7 °C to be stable under atmospheric pressure or require a pressure of 4 MPa to be stable at 4 °C (Sloan and Koh, 2008). The controlled synthesis of methane hydrates from the aqueous phase is additionally difficult, mainly because of the low solubility of methane in water ($1.5 \cdot 10^{-3}$ mol methane per 1 mol water at 5 MPa and 25 °C (Lide and Frederikse, 1995). This low solubility necessitates extensive pore fluid circulation and long experimental time for hydrate formation from the aqueous phase (Spangenberg et al., 2005).

We used Tetrahydrofuran (THF) which forms hydrates at atmospheric pressure and temperatures of 4 °C (Sloan and Koh, 2008). THF is a heterocyclic ether with the molecular formula C_4H_8O. THF is completely miscible in water (Sloan and Koh, 2008) and thus widely used to resemble hydrate formation from methane dissolved in water (Pearson et al., 1986; Collett and Ladd, 2000; Yun et al., 2005). Lee et al. (2007) demonstrated that THF and methane hydrates exhibit similar macroscale mechanical, electrical and thermal characteristics. THF has the advantage of providing close control on the hydrate saturation by varying the stoichiometric THF-H_2O mixture without having the long formation history of methane hydrates. However, it should be noted that THF forms structure-II hydrates whereas pure methane forms structure-I hydrates. Hydrates in nature, especially when formed from thermogenic gas, often contain longer chain hydrocarbons (e.g. ethane, propane) in addition to methane and thus can form structure-II hydrates (Sloan and Koh, 2008) . Therefore, THF hydrates are
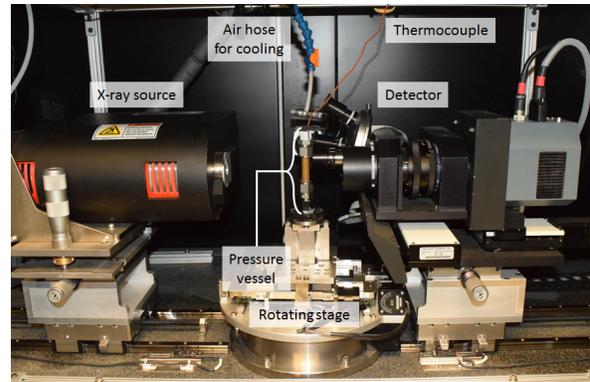

Figure 2: Experimental setup inside the CT scanner

used as a proxy for naturally occurring gas hydrates.

EXPERIMENTAL METHOD

MXCT imaging was performed in the MicroXCT-400 apparatus from XRadia. A Torlon (polyamide-imide) pressure cell with stainless steel fittings on both ends was used. The pressure cell has an inner diameter of 7 mm and a length of 8 cm (Figure 2). The setup was temperature controlled by cooled air. Air from a compressor is transported through a copper coil located in a cooling bath ($T_{bath} = -30°C$) and then led through a thermally insulated hose into the CT apparatus. The insulated section between cooling bath and CT apparatus also contains a hose loop which circulates cooled ethylene glycole alongside the air hose for additional cooling. This setup provides cooling to temperatures as low as 1 °C for periods of multiple days to keep the hydrates stable while high-resolution CT scans are performed.

Samples were formed directly in the pressure vessel and had a volume of approximately 3 ml. Sample components were unconsolidated borosilicate glass beads (diameter: 1 mm) used as host sediment, de-ionized water, THF and barium chloride. Stoichiometric mixtures of THF and water were used to obtain hydrate saturations of 40%, 60% and 80%. Barium chloride was added to achieve a density contrast between THF hydrates and residual brine. The specimen exhibited a porosity of approximately 0.35. The porosity was determined from CT images. After combining all sample compounds, the sample was cooled to approximately 1 °C. The temperature was constantly kept above 0 °C to avoid the formation of ice along with THF hydrates.

MXCT measurements allow the distinction between materials based on their bulk densities. They provide insight into the distribution of different sample components in the pore space. In contrast to sediment grains, glass beads have a uniform X-ray absorbance value, shape and density (2.23 g/cm^3). These properties make it easier to interpret the MXCT images. The output data of the MXCT apparatus are gray scale images. Different gray values represent materials with different bulk densities (high density:light gray, low density: dark gray).
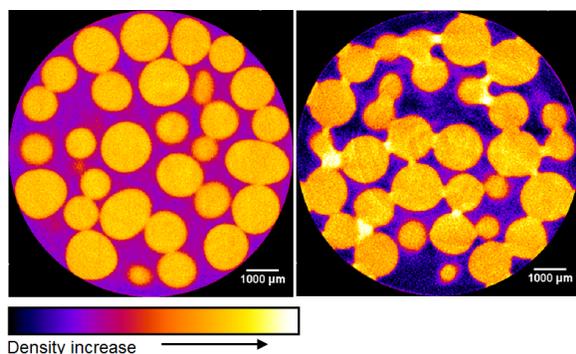
Rock physics of hydrate-bearing sediments

Figure 3: CT images showing horizontal slice through a glass-bead sample. Left: pore space filled with THF, water and barium chloride at room temperature, right: pore space filled with THF hydrate (S_h=80%), barium chloride and barium chloride brine. Resolution of 14.9 μm. White/light yellow: barium chloride precipitate, yellow/orange: glass beads, pink/violet: barium chloride brine, dark violet/black: THF hydrates

Barium chloride was added to the fluid mixture to enhance the density contrast between residual water and hydrates. As hydrates form, barium chloride is excluded from the hydrate structure and remains within the water phase The bulk densities of each sample component are listed in Table 1. The amount of barium chloride was adjusted for each sample in order to obtain a density of 1.1 g/cm^3 for the remaining water assuming that all THF in the sample has been converted to hydrates.

In this study, the hydrate-bearing samples were monitored after the hydrate-formation process was completed. MXCT imaging of THF hydrate dissociation was discussed in Schindler and Batzle (2014). X-ray source voltage of 150 kV and power of 6.2 Watt were used for all tomographies. Magnification of 0.5X (resolution 14.9 μm and 45.4 μm) was used to obtain a big field of view and thus an overview over the sample, magnification of 4X (resolution 5 μm) was used for a detailed view of the pore space. Best results were obtained for angular increments of 0.1° to 0.2° resulting in scanning durations of 1.5 to 6 hours.

RESULTS

The reconstructed CT images (Figure 3) contain information about the distribution of different components of the sample. Different gray values in the CT images represent different densities in the sample. For better visualization high densities are shown in light yellow, intermediate densities are represented by orange and pink areas and low densities are shown in violet and black. Because of its low density (Table 1), THF hydrates and ice appear as violet and black areas in the CT image whereas barium chloride brine and precipitated barium chloride appear in light yellow caused by their higher density (Table 1).

Figure 3 shows CT images for a sample with 80% hydrate saturation. The images indicate that THF hydrates are located in

Table 1: Density of sample components for hydrate saturation $S_h = 80\%$ and addition of 3.2 wt% BaCl$_2$

Component	Density [g/cm^3]
water	1.00
BaCl$_2$	3.84
BaCl$_2$ brine (12.3 wt%)	1.1
THF hydrate	0.97
THF-water-BaCl$_2$ mixture	1.00

the pore body with little to no contact to the grain surfaces. Barium chloride precipitate is found at the grain contacts and fills some small pores entirely. Glass bead surfaces are covered with a layer of barium chloride brine. From these observations we conclude that THF hydrates can contribute to seismic and acoustic velocities as explained by the pore-filling model of the effective medium theory. The presence of hydrates causes an increase in sediment stiffness and thus in seismic velocities. The observation of salt precipitate at grain contacts would lead to a further increase in velocities compared to the pore filling effective medium model which only considers the presence of THF hydrates.

CONCLUSIONS

Micro X-ray computed tomography observations indicate that hydrates from water-THF-solution form in the pore body, away from the grain surfaces. The grain surfaces are covered with a film of barium chloride brine indicating that THF hydrates are the non-wetting phase and forms according to the pore-filling model with salt cementing the sediment grains. Due to the high flux of water in natural sediments, salt precipitation is unlikely to occur in natural gas hydrate reservoirs. However, the effect of salt cementation needs to be taken into consideration for laboratory studies involving salt in hydrate-bearing samples.

Given that THF hydrate is a proxy for one possible texture of natural occurring hydrate, we conclude that natural gas hydrate in coarse grained sediments is primarily non-cementing when formed from natural gas dissolved in water. This conclusion is essential for the assessment of gas hydrate saturation from seismic and well log data.

ACKNOWLEDGEMENTS

Rock physics of hydrate-bearing sediments

REFERENCES

Anderson, B. J., J. W. Wilder, M. Kurihara, M. D. White, G. J. Moridis, S. J. Wilson, M. Pooladi-Darvish, Y. Masuda, T. S. Collett, R. B. Hunter, et al., 2008, Analysis of modular dynamic formation test results from the mount elbert 01 stratigraphic test well, milne point unit, north slope, alaska: British Columbia, Canada.

Boswell, R., and T. S. Collett, 2006, Fire in the ice: The gas hydrates resource pyramid.

Collett, T. S., A. H. Johnson, C. C. Knapp, and R. Boswell, 2009, Natural gas hydrates: A review: Natural gas hydrates - Energy resource potential and associated geologic hazards: AAPG Memoir, **89**, 146–219.

Collett, T. S., and J. Ladd, 2000, Detection of gas hydrate with downhole logs and assessment of gas hydrate concentrations (saturations) and gas volumes on the blake ridge with electrical resistivity log data: **164**, 179–191.

Collett, T. S., and M. W. Lee, 2012, Well Log Characterization of Natural Gas Hydrates 1: **53**, 348–367.

Dallimore, S. R., J. F. Wright, F. M. Nixon, M. Kurihara, K. Yamamoto, K. Fuji, M. Numasawa, M. Yasuda, and Y. Imasato, 2008, Geologic and porous media factors affecting the 2007 production response characteristics of the jogmec/nrcan/aurora mallik gas hydrate production research well: Presented at the Proceedings of the 6th International Conference on Gas Hydrates.

Dobrynin, V. M., Y. P. Korotajev, and D. V. Plyuschev, 1981, Gas hydrates - a possible energy resource: Pitman Publishers, Boston.

Ecker, C., J. Dvorkin, and A. Nur, 1998, Sediments with gas hydrates: Internal structure from seismic AVO: Geophysics, **63**, 1659–1669.

Helgerud, M. B., J. Dvorkin, A. Nur, A. Sakai, and T. S. Collett, 1999, Elastic-wave velocity in marine sediments with gas hydrates: Effective medium modeling: Geophysical Research Letters, **26**, 2021–2024.

Kerkar, P. B., K. Horvat, K. W. Jones, and D. Mahajan, 2014, Imaging methane hydrates growth dynamics in porous media using synchrotron x-ray computed microtomography: Geochemistry, Geophysics, Geosystems, **15**, 4759–4768.

Kunerth, D. C., D. M. Weinberg, J. W. Rector, C. L. Scott, and J. T. Johnson, 2001, Acoustic laboratory measurements during the formation of a thf-hydrate in unconsolidated porous media: Journal of seismic exploration, **9**, 337–354.

Lee, J. Y., T. S. Yun, J. C. Santamarina, and C. Ruppel, 2007, Observations related to tetrahydrofuran and methane hydrates for laboratory studies of hydrate-bearing sediments: Geochemistry, Geophysics, Geosystems, **8**.

Lide, D. R., and H. P. R. Frederikse, 1995, Crc handbook of chemistry and physics.

Meyer, R. F., 1981, Speculations on oil and gas resources in small fields and unconventional deposits: Long-term Energy Resources, **1**, 49–72.

Pearson, C., J. Murphy, and R. Hermes, 1986, Acoustic and resistivity measurements on rock samples containing tetrahydrofuran hydrates: laboratory analogues to natural gas hydrate deposits: Journal of Geophysical Research: Solid Earth, **91**, 14132–14138.

Priest, J. A., A. I. Best, and C. R. I. Clayton, 2005, A laboratory investigation into the seismic velocities of methane gas hydrate-bearing sand: Journal of Geophysical Research: Solid Earth, **110**.

Rydzy, M. B., and M. L. Batzle, 2011, Rock physics characterization of THF hydrate-bearing sediment: Presented at the Proceedings of the 7th International Conference on Gas Hydrates.

Schindler, M., and M. L. Batzle, 2014, Pore-scale investigation of hydrate-bearing sediments, *in* Poate, J. M., H. Kazemi, T. H. Illangasekare, and R. J. Kee, eds., Pore Scale Phenomena - Frontiers in Energy and Environment, World Scientific.

Sloan, E. D., and C. A. Koh, 2008, Clathrate hydrates of natural gases: CRC press.

Spangenberg, E., J. Kulenkampff, R. Naumann, and J. Erzinger, 2005, Pore space hydrate formation in a glass bead sample from methane dissolved in water: Geophysical Research Letters, **32**.

Waite, W. F., W. J. Winters, and D. H. Mason, 2004, Methane hydrate formation in partially water-saturated ottawa sand: American Mineralogist, **89**, 1202–1207.

Yun, T. S., F. M. Francisca, J. C. Santamarina, and C. Ruppel, 2005, Compressional and shear wave velocities in uncemented sediment containing gas hydrate: Geophysical Research Letters, **32**.

REFERENCES

Anderson, B. J., J. W. Wilder, M. Kurihara, M. D. White, G. J. Moridis, S. J. Wilson, M. Pooladi-Darvish, Y. Masuda, T. S. Collett, and R. B. Hunter, 2008, Analysis of modular dynamic formation test results from the Mount Elbert 01 stratigraphic test well, milne point unit, North Slope, Alaska: British Columbia, Canada.

Boswell, R., and T. S. Collett, 2006, Fire in the ice: The gas hydrates resource pyramid.

Collett, T. S., A. H. Johnson, C. C. Knapp, and R. Boswell, 2009, Natural gas hydrates: A review: Natural gas hydrates – Energy resource potential and associated geologic hazards: AAPG Memoir, 89, 146–219.

Collett, T. S., and J. Ladd, 2000, Detection of gas hydrate with downhole logs and assessment of gas hydrate concentrations (saturations) and gas volumes on the Blake Ridge with electrical resistivity log data: Proceedings of the Ocean Drilling Program: Scientific Results, 164, 179–191.

Collett, T. S., and M. W. Lee, 2012, Well log characterization of natural gas hydrates: SPWLA, **1**, no. 53, 348–367.

Dallimore, S. R., J. F. Wright, F. M. Nixon, M. Kurihara, K. Yamamoto, K. Fuji, M. Numasawa, M. Yasuda, and Y. Imasato, 2008, Geologic and porous media factors affecting the 2007 production response characteristics of the Jogmec/Nrcan/Aurora Mallik gas hydrate production research well: Presented at the Proceedings of the Sixth International Conference on Gas Hydrates.

Dobrynin, V. M., Y. P. Korotajev, and D. V. Plyuschev, 1981, Gas hydrates — A possible energy resource: Pitman Publishers.

Ecker, C., J. Dvorkin, and A. Nur, 1998, Sediments with gas hydrates: Internal structure from seismic AVO: Geophysics, **63**, 1659–1669.

Helgerud, M. B., J. Dvorkin, A. Nur, A. Sakai, and T. S. Collett, 1999, Elastic-wave velocity in marine sediments with gas hydrates: Geophysical Research Letters, **26**, no. 13, 2021–2024.

Helgerud, M. B., J. Dvorkin, A. Nur, A. Sakai, and T. Collett, 1999, Effective medium modeling: Geophysical Research Letters, **26**, no. 13, 2021–2024. http://dx.doi.org/10.1029/1999GL900421.

Kerkar, P. B., K. Horvat, K. W. Jones, and D. Mahajan, 2014, Imaging methane hydrates growth dynamics in porous media using synchrotron X-ray computed microtomography: Geochemistry Geophysics Geosystems, **15**, no. 12, 4759–4768. http://dx.doi.org/10.1002/2014GC005373.

Kunerth, D. C., D. M. Weinberg, J. W. Rector, C. L. Scott, and J. T. Johnson, 2001, Acoustic laboratory measurements during the formation of a THF-hydrate in unconsolidated porous media: Journal of seismic exploration, **9**, 337–354.

Lee, J. Y., T. S. Yun, J. C. Santamarina, and C. Ruppel, 2007, Observations related to tetrahydrofuran and methane hydrates for laboratory studies of hydrate-bearing sediments: Geochemistry, Geophysics, Geosystems, 8.

Lide, D. R., and H. P. R. Frederikse, 1995, CRC handbook of chemistry and physics: Taylor and Francis Group, LLC.

Meyer, R. F., 1981, Speculations on oil and gas resources in small fields and unconventional deposits: Long-term Energy Resources, **1**, 49–72.

Pearson, C., J. Murphy, and R. Hermes, 1986, Hydrates: Laboratory analogues to natural gas hydrate deposits: Journal of Geophysical Research. Solid Earth, **91**, no. B14, 14132–14138. http://dx.doi.org/10.1029/JB091iB14p14132.

Priest, J. A., A. I. Best, and C. R. I. Clayton, 2005, A laboratory investigation into the seismic velocities of methane gas hydrate-bearing sand: Journal of Geophysical Research: Solid Earth, 110.

Rydzy, M. B., and M. L. Batzle, 2011, Rock physics characterization of THF hydrate-bearing sediment: Proceedings of the Seventh International Conference on Gas Hydrates.

Schindler, M., and M. L. Batzle, 2014, Pore-scale investigation of hydrate-bearing sediments, *in* J. M. Poate, H. Kazemi, T. H. Illangasekare, and R. J. Kee, eds., Pore scale phenomena — Frontiers in energy and environment: World Scientific.

Sloan, E. D., and C. A. Koh, 2008, Clathrate hydrates of natural gases: CRC Press.

Spangenberg, E., J. Kulenkampff, R. Naumann, and J. Erzinger, 2005, Pore space hydrate formation in a glass bead sample from methane dissolved in water: Geophysical Research Letters, 32.

Waite, W. F.,W. J. Winters, and D. H. Mason, 2004, Methane hydrate formation in partially water-saturated Ottawa sand: American Mineralogist, **89**, 1202–1207.

Yun, T. S., F. M. Francisca, J. C. Santamarina, and C. Ruppel, 2005, Compressional and shear-wave velocities in uncemented sediment containing gas hydrate: Geophysical Research Letters, 32.